



Current status of imaging of Sjogren's syndrome

Sandrine Jousse-Joulin, Guillaume Coiffier

► To cite this version:

Sandrine Jousse-Joulin, Guillaume Coiffier. Current status of imaging of Sjogren's syndrome. Best Practice and Research: Clinical Rheumatology, 2020, 34, pp.101592 -. <10.1016/j.berh.2020.101592>. <hal-03493766>

HAL Id: hal-03493766

<https://hal.science/hal-03493766v1>

Submitted on 16 Dec 2022

HAL is a multi-disciplinary open access archive for the deposit and dissemination of scientific research documents, whether they are published or not. The documents may come from teaching and research institutions in France or abroad, or from public or private research centers.

L'archive ouverte pluridisciplinaire **HAL**, est destinée au dépôt et à la diffusion de documents scientifiques de niveau recherche, publiés ou non, émanant des établissements d'enseignement et de recherche français ou étrangers, des laboratoires publics ou privés.



Distributed under a Creative Commons CC BY-NC 4.0 - Attribution - Non-commercial use - International License

Current status of imaging of Sjogren's syndrome.

Sandrine Jousse-Joulin^{1*}, Guillaume Coiffier².

1. Rheumatology department, CHU de Brest, Univ Brest, Inserm, LBAI, UMR1227, Brest, France
2. Rheumatology department, CHU de Rennes, Hôpital Sud, 16 boulevard de Bulgarie, BP 90347, 35203 Rennes, France.

*corresponding author sandrine.jousse-joulin@chu-brest.fr

Abstract

Primary sjögren's syndrome (pSS) is an autoimmune disease which involves salivary glands and extra glandular organs. Today, Sjögren's patients' diagnosis is based on classification criteria taking into account five objective tests, including histology, immunology, two ophthalmologic tests, and salivary flow evaluation. To date, the challenge is to find the right imaging tool for diagnosis, follow up and prognosis of pSS. The objective of this review is to describe what are these imaging modalities and especially the place and validity of salivary glands ultrasonography (SGUS) in the diagnosis and follow-up strategy of patients with suspected pSS. Moreover, new non-invasive tools are emerging, including elastography a new ultrasonography technique that provides an estimate of tissue elasticity, MRI, MR sialography, and ¹⁸Fluorodeoxyglucose–Positron Emission Tomography. Although new imaging opportunities are available, SGUS should be the first-line choice in pSS because of its accessibility, feasibility over time, and sensitivity to change.

Key words: salivary glands, ultrasonography, Sjögren's syndrome, elastography, MRI,

¹⁸Fluorodeoxyglucose–Positron Emission Tomography

1. Introduction

Ultrasound (US) is an upcoming imaging technique in rheumatology and shows usefulness in evaluating salivary glands (SG) in primary Sjögren's syndrome (pSS) patients. Nonetheless, the use of salivary glands ultrasonography (SGUS) for diagnosis and prognosis considerations in pSS is not yet fully integrated into the daily practice of many rheumatologists. Currently, SGUS is still only considered as a research tool, especially until the operator has demonstrated his competence and reliability.

To date, the pSS diagnosis is based on classification criteria, which have been revisited since 2002 (1). In 2012, the American College of Rheumatology (ACR) suggested an alternative version of the criteria first proposed by the American-European Consensus Group (AECG), based on the Sjögren's international collaborative clinical alliance (SICCA) cohort, and almost excluding oral and salivary components, except for minor salivary gland biopsy (MSGB) and sialometry (2). Then, in 2016 a new set of classification criteria for pSS was presented, based on 5 objective tests or items, resulting in a total score ≥ 4 (3). In these new criteria, the involvement of SGs is documented by unstimulated salivary flow (USF) and/or the MSGB. Despite the constant development and validation of new promising imaging techniques such as SGUS, their implementation as the first line of imaging tools for diagnosis and/or follow up of pSS patients is under debate, especially concerning SGUS.

The objective of this narrative review is to discuss the validity and place of SG imaging, especially SGUS, in the diagnostic and follow-up strategy of patients with suspected pSS.

2. How is SGUS imaging being used as an outcome measure in Sjogren's syndrome?

In order to be used as an outcome measure, the metric properties of SGUS have to be validated.

2.1. *Criterion measure of truth validity*

In 2016 OMERACT metric properties (truth, discrimination, and feasibility) of SGUS in pSS patients have been studied in a systematic literature review (4). In summary, only the criterion measure of truth validity (*i.e.*, comparison between parotid and submandibular gland US results with those of biopsy) were not validated as well as discriminant validity (*i.e.*, reliability between ultrasonographers). Since then, these 2 OMERACT pillars have been validated.

On the contrary, construct measure of truth validity (*i.e.*, comparison of SGUS to other imaging techniques) has been validated, showing the superiority of SGUS to sialography, but with less sensitivity in comparison with MRI for detecting parenchymal inhomogeneity, particularly in early stages of the disease. MSGB was used in most studies as the reference standard to assess the truth validity of SGUS. A good indirect correlation was found between SGUS and biopsy. Agreement between parotid gland (PG) US and PG biopsy was investigated in a cohort of 103 outpatients with suspected pSS (5). In this study, the

absolute agreement between parotid SGUS and parotid biopsy was 83% (65/78), confirming that abnormal ultrasound findings corresponded to abnormal histological features.

In this cohort, only 43 out of 103 pSS patients underwent both PG biopsy and MSGB. The correlation between MSGB findings and total SGUS score was moderate and slightly better ($R = 0.412$) than for PG biopsy ($R = 0.376$) (6,7). Similarly, the TEARS trial showed a good correlation coefficient between the global SGUS grade and the focus score of MSGB ($R = 0.612$) (8,9).

Furthermore, Theander *et al.* highlighted that SGUS scores of 2 or 3 were associated with clinical, serological, histological, and cytologic markers of lymphoma risk, namely germinal center-like structures on MSGB, CD4 lymphopenia and reduced number of memory B cells in blood samples (10). More recently, we suggested that alteration of major SG assessed by SGUS could be associated with cryoglobulinemic vasculitis and lymphoma in pSS. We especially highlighted that only the following high levels of echostructural changes should be closely monitored, which included either numerous cystic lesions without healthy parenchyma or fibrous glands scored as a grade 3 according to the new semi-quantitative scoring system as described by the SG-US OMERACT task force (12).

2.2. Reliability measure of discriminant validity

The previous systematic literature review has failed to identify any robust evaluations of the reliability of SGUS in pSS (4). Indeed, just three studies have evaluated inter-observer reliabilities out of 12 with only two readers and only on static images. Since, Damjanov *et al.* published a SGUS reliability exercise between 2 European centers with patients (Serbia and Spain), including 5 and 8 observers respectively, that demonstrated good reliability regarding the homogeneity of SG as primary evaluation criteria (13).

More recently, the USpSS-EULAR group established a SGUS atlas in pSS patients and a two steps reliability exercise: one based on static images and one based on acquisition images (12). This group highlighted that reliability evaluation on static images showed that the most reliable parotid gland abnormalities were homogeneity (mean kappa, 0.76), the number and location of hypo/anechoic foci (mean kappa, 0.78). Concerning the submandibular glands (SMG), the reliability of these abnormalities was also substantial (homogeneity: mean kappa, 0.63; hypoechoic/anechoic foci: mean kappa, 0.76; and location: mean kappa, 0.69). During acquisition, good reliability was found concerning parotid gland for homogeneity (mean kappa, 0.66) and for number (mean kappa, 0.74) and location (mean kappa, 0.77) of hypo/anechoic foci, whereas reliability was only moderate for these findings at the SMG (12).

Regarding sensitivity to change, the measure of discriminant validity, three studies have been published and showed a SGUS change with treatment (14-16). Consequently, use of SGUS was able to demonstrate disease modification after treatment with rituximab.

These data strongly support the inclusion of SGUS in future classification and diagnostic criteria.

3. How to use SGUS in daily practice? What are the data concerning its clinical relevance for the diagnosis, the prediction of onset, and the complications of the disease?

3.1. What are the elementary SGUS lesions for the diagnosis of pSS?

Elementary US lesions in B-mode have been known since the 1990s (17,18), without any new description since then, despite the significant improvement in the performances of the available US-devices. A large number of abnormalities can be investigated and observed on SGUS during pSS: changes in size (often parotidomegaly and atrophy of the submandibular gland), the disappearance of the posterior border of the gland or all gland borders in comparison with the surrounding tissues, heterogeneity of the parenchyma with hypoechoic areas often described as pseudo-cystic lesions, hyperechoic bands, and/or multiple calcifications or aggregates. These lesions have recently been the subject of consensus definitions (19).

All of these lesions may be present in varying proportions and co-exist in a patient with pSS. Moreover, these different lesions correspond to different anatomical changes occurring during the different stages of the disease.

The hypoechoic areas (without pseudocyst), which is responsible for the heterogeneity of the parenchyma of the glands, correspond to an infiltration of the gland by inflammatory cells and/or also of fat depositions within the gland, a feature which is probably best assessed by MRI (20).

The pseudocysts correspond to the ectasia of the lobular salivary ducts secondary to the inflammatory infiltrate, and their number and size are proportional to what is observed on standard sialography or MRI sialography (20-23). Over time, these pseudocysts may reveal, although not systematically, small punctiform aggregates (17). At this point, the salivary gland can be destroyed, leading to a diffuse, almost complete adipose infiltration. This fatty evaluation is responsible for the disappearance of gland borders that become imperceptible from the gland surrounding tissues on US evaluation. At this stage, gland parenchyma is also characterized by the presence of hyperechoic bands secondary to post-inflammatory fibrosis (24).

Mostly, all major SGs are affected by this phenomenon, but different stages can be simultaneously observed on the different glands of the same patient. Parenchymal involvement of an isolated salivary gland should suggest a differential diagnosis and is not in favor of pSS diagnosis. Although Mossel *et al.* (25) suggested that only one side (one parotid and submandibular gland) could be performed with the same diagnostic performance as the four major SG study for assessment during pSS, we believe that it is necessary for clinical practice to evaluate the four major SGs because of the possible differential etiologies as we will describe later on in this review. In addition, parenchymal destruction in the context of chronic lithiasis may give rise to the same elementary lesions, as described in pSS (26).

3.2. What are the different scoring strategies of SGUS evaluation for pSS?

Since the description of these various elementary lesions by DeVita *et al.* in 1992 (17), a large number of classifications have been proposed for scoring the SGUS damages observed during pSS (10,12,17,18,24,27-30). Heterogeneity of the parenchyma is the essential anomaly found in all scoring systems. Some scores also characterize and grade pseudocystic lesions (number and size). Other scores also focus on hyperechoic fibrous bands. Punctiform aggregates are generally not used in most of the scoring strategies proposed so far. All different SGUS scoring strategies are described in **Table 1**.

3.3. What is the diagnostic performance of these different SGUS scoring strategies?

The sensitivity of the SGUS was variable, ranging from 63-95% in different studies. Specificity was generally better between 80 and 95%. Variations in performance were explained by a different scoring system and pathological thresholds depending on the studies(4). Three studies have compared different SGUS scoring without showing any significant differences in the diagnostic performances of the considered scores (31-33).

Several studies have shown good diagnostic performance and significant positive correlations of the diagnosis based on SGUS with sialography (20-22). Some authors have suggested replacing sialography (an invasive examination) included in the AECG criteria for Sjögren classification by SGUS (22, 34, and 35). Nonetheless, sialography was finally not included in the ACR/EULAR classification criteria (neither 2012 nor 2016), and no salivary gland imaging technique was included in this classification (2, 3). Therefore, it appeared important to reach a consensus for the most relevant and reliable scoring strategy of SGUS evaluation for pSS, to foster its use in daily practice but also to study its weight compared to other clinical, immunological, histological and functional variables included in the ACR/EULAR 2016 classification criteria (36-40).

Based on data from the literature, a group of experts has validated the elementary abnormal lesions to be studied by SGUS and has proposed an international consensus scoring strategy following the OMERACT recommendations. This SGUS OMERACT-score is detailed in **Figure 1** (12,19).

Recently, the SGUS OMERACT-score has shown its association with the diagnosis of pSS, independently from other criteria (anti-SSA antibodies, histological findings with focus score ≥ 1 in MSGB, or salivary/lacrymal functional test) that are included in the ACR 2016 classification (40).

All studies incorporating SGUS in existing classification criteria have reported an improvement of sensitivity and a slight decrease of specificity, regardless of the considered pSS classification (34-40).

Currently, it is proposed that SGUS is the first-line morphological examination to be carried out in the case of clinical suspicion of pSS, in addition to immunological (anti-SSA antibodies), functional (Shirmer Test and saliva flow) and histological data. However, histology is an invasive technique and an abnormal SGUS with an OMERACT score of 2 should increase the diagnostic confidence of making a diagnosis of Sjogren's syndrome.

3.4. Is SGUS associated with sicca syndrome (subjective and functional impairment)?

A strong positive correlation between salivary flow and ultrasound score of major salivary glands was reported in all studies. For example, the authors observed lower unstimulated salivary flow (0.8 ml vs 1.9 ml/15 min, $p < 0.01$) ($r = -0.424$) or salivary flow after stimulation (3.4 ml vs 6.7 ml/min, $p < 0.01$) ($r = -0.503$) in pSS patients ($n = 94$) with a high SGUS score compared to those with no/non-specific ultrasound abnormalities, respectively (41). A similar result was observed for the lacrimal production explored by the Shirmer test with lower correlation values (41). When considering the different US elementary lesions, Zabotti *et al.* (42) pointed out abnormalities of unstimulated salivary flow measurements were independently associated with hyperechogenic bands. The association with the ESSPRI score was inconsistent across studies (43,44). Nevertheless, ESSPRI contains a VAS scale for the evaluation of asthenia and does not exclusively evaluate sicca syndrome. Moreover, Hammenfors *et al.* (41) reported a positive correlation between the VAS scale oral sicca syndrome and the severity score of USSG.

3.5. Is the US-SG a predictive tool during pSS?

The burden of pSS is mainly due to its bothersome symptoms: asthenia, sicca syndrome, and musculoskeletal pain. But the disease can also lead to serious complications i) due to the development of cryoglobulinemic vasculitis and/or non-Hodgkin's B malignant lymphoma, or ii) due to visceral involvement (mainly CNS but also pulmonary, renal or muscular impairment).

Therefore, it appears important to have predictive markers for the occurrence of these serious complications to improve patients' follow-up. Unfortunately, we have not yet available longitudinal data to evaluate the value of SGUS as a predictive tool, but a large number of associations between ultrasound and severity markers suggest its potential usefulness. Indeed, several cross-sectional studies have clearly shown that the severity of parenchyma involvement based on SGUS evaluation was associated with high levels of histological infiltrate (45-47), ESSDAI disease activity (43) or even specific complications such as cryoglobulinemic vasculitis and/or B-lymphoma (11,43).

3.6. Could the SGUS be useful to guide therapeutic strategy in pSS?

Unfortunately, most immunomodulatory therapies have failed to show efficacy during pSS, especially on sicca syndrome symptoms. Most of the time, the explanations put forward is the lack of activity score sensitive to change during the pSS or a lack of relevant selection criteria based on pSS specific phenotypes and/or subgroups. Could SGUS be a phenotyping tool for selecting patients who might benefit the most from specific treatments?

Cornec *et al.* (48) reported that a low baseline SGUS score was associated with sicca-related outcomes improvement after treatment with rituximab (TEARS study). The median total SGUS grade at inclusion was 9 [6-11] in responders versus 16 [11-16] in non-responders ($p = 0.04$). The proportion of SSRI-30 responders was 0% among patients with SGUS grade 4, while 88% among those with \leq SGUS grade 3.

In the same study, parotid parenchymal echo-structure improved in 50% of the rituximab-treated patients versus 7% of the placebo-treated patients ($p = 0.03$). In the submandibular glands, echo-structure also improved in a larger proportion of rituximab-treated patients, although the difference was not significant (36% versus 7% of placebo-treated patients; $p = 0.16$) (15).

A second RCT evaluating the effects of rituximab versus placebo (TRACTISS) reported similar results. SGUS composite index improved in the rituximab arm with an OR of 6.8 (95% CI 1.1 to 43.0; $p=0.04$) at week 16 and 10.3 (95% CI 1.0 to 105.9; $p=0.05$) at week 48 . The total SGUS score improved significantly in the rituximab group compared to the placebo group, and the significant difference occurred for posterior border visibility (16).

These results are particularly encouraging because it was shown that the heterogeneity of the parenchyma of the salivary glands was not changed between two ultrasound examinations carried out two years interval during the natural history of the disease without treatment (49).

3.7. What added value does Doppler assessment offer to SGUS in pSS?

The vascularization of salivary glands (SG) in pSS has not been extensively studied by imaging techniques, and currently, no agreement exists on how this should be best evaluated.

Color Doppler ultrasonography (CDUS) might represent an interesting tool for the assessment of vascularization in SS. In five studies, the CDUS signal was used to determine resistive index to assess SG vascularisation (14,15,50-52). CDUS evaluation of the facial artery that vascularizes the SMG appears to be the most efficient. In normal conditions, the flow is modified after salivary stimulation with lemon juice, responsible for an aliasing artifact, and a significant decrease of the resistivity index (53). In patients with pSS, the waveform showed systolic-diastolic flow with a reduction in the resistivity index, suggesting the presence of downstream hypervascularization (inflammatory vasodilation arteries of the salivary glands) with no or few modifications after salivary stimulation. However, no reproducible pathological threshold for resistance index or systolic peak have been defined for their use in clinical practice (52).

Power Doppler was only used in one study based on the counting of spots in the region of interest. Hypervascularization is generally a diffused pattern, deriving from the presence of small vessels, both peripheral and randomly distributed inside the SG, visible as punctiform signals in the early stage of the pSS (51). However, a reduction in glandular volume associated with hypo-vascularisation was also described for later stages (54).

Contrast-enhanced CDUS was used in one study and demonstrated a significant difference between pSS and secondary SS during lemon stimulation, with lower value in the pSS group (55).

Interestingly, some studies (14,15) have evaluated the relevance of CDUS as an outcome measure of response to therapy, but with inconsistent results. A first study (14) showed improvement of the SG parenchymal vascularization in patients treated with rituximab while there was no change with the same treatment in a second one (15). Nonetheless, none of these studies evaluated the reliability of their

Doppler evaluating strategy for the assessment of salivary gland involvement according to the OMERACT standards.

Recently, a subtask force of the OMERACT working group performed a reliability exercise among nine ultrasonographers with expertise on the vascularization of salivary glands in patients with Sjögren's syndrome and showed good to excellent intra-reliability and good inter-reliability using a new semi-quantitative CDUS scoring system (Grade 0, no visible vascular signals; Grade 1, focal, dispersed vascular signals; Grade 2, diffuse vascular signals detected in less than 50% of the gland; Grade 3, diffuse vascular signals in more than 50% of the gland) (56).

Therefore, CDUS could be a future useful imaging technique to evaluate activity of pSS and response to treatment.

3.8. What added value does elastography offer to SGUS in pSS?

Ultrasound elastography (USE) is an imaging technology sensitive to tissue stiffness that was first described in the early 1990s. USE assesses tissue elasticity, which is the ability of tissue to resist the deformation induced by an applied force and/or to return to its original shape after removal of the force. Two main techniques are available: strain imaging and shear wave imaging.

In strain imaging, tissue displacement is measured by the correlation of Repetition Frequency (RF) echo signals between search windows before and after compression. Two USE based-approaches exist for strain imaging: Real-Time Tissue Elastography (RTTE) and Acoustic Radiation Force Impulse (ARFI) strain imaging (57,58).

In shear wave imaging, the initial paradigm is that particle motion is perpendicular to the direction of wave propagation, with shear wave speed related to the shear modulus. Dynamic stress is applied to tissue by using a mechanical vibrating device in 1D transient elastography (1D-TE) or acoustic radiation force in point shear wave elastography (pSWE) and 2D shear wave elastography (2D-SWE). The advantages of 2D-SWE include real-time visualization of a color quantitative elastogram superimposed on a B-mode, enabling the operator to be guided by both anatomical and tissue stiffness information (58). This is particularly important given the heterogeneity of salivary parenchyma in pSS.

Since 2014, twelve studies have evaluated the performance of USE for the diagnosis of pSS (**Table 2**) (59-71). All these studies have shown a loss of glandular elasticity during the pSS, particularly in the PGs. RTTE techniques seem insufficient for a correct evaluation of SG (59,60,64,66). ARFI techniques were most often evaluated, showing a sensitivity between 77 and 92% with a highly variable specificity between 50 and 92% (61-66,68). These large variations in ARFI performance depended mainly on the chosen SWE (m/s) thresholds, but also on the nature of the control group (including healthy subjects, sicca syndrome without pSS or other inflammatory pathologies of SG), which could lead lower specificity. However, these performances remained lower than those of the SGUS in B mode.

Nevertheless, USE performance seems to be improved thanks to the 2D-SWE technique (69,70). Interestingly, a recent study reported the usefulness of the 2D-SWE technique in the subgroup of patients

with normal (Grade 0) or indeterminate (Grade 1) in B-mode SGUS evaluation, allowing a more confident and robust diagnosis of pSS (in accordance with the ACR 2016 classification) with 94% of cases showing an elasticity ≥ 6.45 kPa (70). Moreover, in this study including eight patients with pSS-related MALT lymphoma, the authors reported that the association of a Grade 3 in SGUS ($> 50\%$ hyperechoic bands) with parotid hypertrophy and elasticity ≥ 11.5 kPa was specific for MALT lymphoma (Sp=100%) with excellent sensitivity (Se=92%) (70).

3.9. Is SGUS useful for the diagnosis of secondary Sjogren's syndrome?

Several studies have evaluated diagnostic performance for the diagnosis of secondary Sjogren's syndrome, most of the time in the context of rheumatoid arthritis or systemic lupus (31,71). The elementary lesions appear to be the same as in pSS, and the same scoring systems is generally used. Diagnostic performances seem to be globally similar to those of pSS.

Nevertheless, the question remains unclear regarding the particular case of Systemic Sclerosis (SSc). Although it is an autoimmune organ disease that may be associated with an overlap syndrome, the frequency of sicca syndrome appears to be higher in SSc (a fibrosing disease) than in other connective tissue diseases (72). A first study reported that lengths of the parotid and submandibular glands were smaller in patients with SSc (n=25) versus controls (n=45). Moreover, a Cornec score ≥ 2 was observed in only 25% of SSc cases versus 75% of pSS, possibly suggesting specific fibrous damage during SSc. These results suggest that further studies are required on this specific topic of SSc associated sicca syndrome (73).

3.10. Is SGUS altered in other inflammatory conditions affecting the salivary glands?

All previous studies that examined the diagnostic performance of SGUS compared pSS with controls with sicca syndrome of various etiology and severity. However, in clinical practice, other etiologies may be responsible for salivary gland infiltration known as Mickulicz syndrome (*i.e.* sarcoidosis, amyloidosis, IgG4-related disease) (Table 3).

One study compared the SGUS characteristics of major salivary glands according to different etiologies: pSS, sarcoidosis, AL amyloidosis, and a control group. The Hoyer score was significantly higher during pSS compared to the other groups. Hopefully, the diagnostic performance of the SGUS for the diagnosis of pSS was not significantly altered when using this strategy that included in the control group classical differential diagnoses such as sarcoidosis or amyloidosis (74).

In IgG4-related disease, a review of the literature suggested that hypoechoic lesions (pseudocyst) involving preferentially the SMGs (with usual sparing of the PGs) were SGUS features rather specific of this disease (74). However, these sonographic features show a significant overlap with those found in pSS. More specific patterns affecting the SMGs have also been described: reticular pattern (alternating hypoechogenic areas surrounded by a hyperechogenic band with "honeycomb" appearance) and nodular pattern (hypoechogenic mass distorting the contours of the gland) (76).

Salivary gland involvement appears to be an important issue for the identification of different phenotypes of IgG4-related disease. Patients with abnormal SGUS parameters defined a specific phenotypic subgroup of patients who were more frequently women, with allergic symptoms, sicca syndrome with lacrimal gland involvement, with higher serum IgG4 and/or eosinophilia, while organ involvement (*i.e.*, lymph node, retroperitoneal fibrosis, pancreas, biliary system, kidney or aorta) were less represented (77).

In all cases, SGUS appears necessary to guide the localization of histological sampling/biopsies.

4. Beyond Ultrasound, what is the added value of other imaging techniques for the management of pSS?

4.1. MR Imaging in the Sjögren Syndrome.

The diagnostic possibilities of the major salivary glands MRI were discussed in the 1990s (78,79). It is a non-invasive, non-irradiating examination that allows an anatomical study of the major salivary glands (weighted sequence T1 without fat saturation and T2 with fat saturation) but also functional (MRI sialography).

MRI has the advantage of being the standard reference for parotid tumors assessment, particularly lymphoma, which is a feared complication of pSS. Thus, an additional diffusion weighting sequence (DW-MR imaging) must be performed in case of suspicion of lymphoma (80,81). The study of the parotid parenchyma seems sufficient, although the submandibular glands may also be considered (82).

4.1.1. MRI imaging of the normal salivary glands

On the T1-weighted sequence, normal parotid parenchyma appears as a homogeneous intermediate signal (lower than subcutaneous fat) with the exception of salivary vessels and ducts that are characterized by hypointensity signal. Fat-suppressed T2-weighted images highlight the architecture of the gland lobules by decreasing extra-signals from inter-lobular fat tissues.

MRI sialography is based on the concept of hydro-MRI. Hydro-MRI relies on the concept of spontaneous T2-hyperintensity signal of stagnant fluid structures with concomitant signal extinction of adjacent tissues, especially used for cholangio-MRI. MRI sialography has very good performance compared to sialography and has the advantages that no injection of contrast (gadolinium) agent is needed and that it is a non-invasive examination. A normal parotid sialogram usually shows a harmonious arborization of the salivary ducts without any dilatation (83).

4.1.2. What is pSS signature on major salivary glands in MRI?

High-intensity areas on T1-weighted MR images of the glands associated with high-intensity areas on fat-suppressed T2-weighted images are the MRI characteristic aspects of pSS. The intact lobule area (intermediate-signal-intensity area on fat-suppressed T2-weighted images) usually decreases during pSS

(84,85). Foci of salivary ducts ectasia are present in growing numbers from grade 1 to grade 3 and finally disappear due to the destruction of the intra-parotid salivary ducts at the most advanced stage of the disease (grade 4) in MRI sialography (80). Fat areas > 5% associated with a decrease in intact parenchyma replaced by hyperintensity signal ranges in fat-suppressed T2-weighted images (< 90%) with a number of foci of salivary ducts > 6 shown excellent performance for the diagnosis of pSS (Se 96%, Sp 100%) (4,83). Tonami *et al.* (85) have also described 4 grades of severity of sialo-MRI according to sialography findings with a good correlation.

A better sensitivity of sialo-MRI (96%) and anatomical MRI (81%) compared to US-SG (78%) has been reported with high specificity for the diagnosis of pSS (4). Diagnostic performances of MRI for pSS are summarized in **Table 4**. Similar MRI characteristics aspects were found in secondary SS associated with RA (86).

Mucosa-Associated Lymphoid Tissue (MALT) Lymphoma of the parotid gland is a classical complication of pSS. Histological diagnosis is essential. However, MRI is a key examination for diagnostic guidance and local extension assessment. Different aspects of MRI have been described, but the association of solid and cystic lesions are observed in 2/3 of the cases of MALT Lymphoma (87). These lesions are frequently bilateral. DW-MR imaging showed hyperintensity with extremely low apparent diffusion coefficient (ADC) (close to 0.5) for solid components. PET/CT shown less specific abnormalities with various and inconsistent SUV_{max} ranging from 1.3 to 17.7 (mean, 6.3) (88). Dynamic contrast-enhanced MR showed an early gadolinium type 1 enhancement profile (89).

4.2. ¹⁸ Fluorodeoxyglucose–Positron Emission Tomography (¹⁸FDG-PET/CT) imaging in the pSS.

Positron Emission Tomography/Computer Tomography (PET/CT) is a relevant imaging tool to assess inflammatory and auto-immune disease activities. FDG uptake can be frequently observed in pSS and mainly distributed in SG, lymph nodes, and lungs 18F-fluorodeoxyglucose (¹⁸FDG). Because patients with SS are known to have an increased risk for developing B-cell lymphoma, there is a rationale for fostering the role of PET in this condition. However, ¹⁸FDG uptake in the lymph nodes is a common finding in pSS (53% in lymphoma vs 43% without lymphoma without any significant difference) (90). Its interpretation should, therefore, be especially cautious in patients with pSS, and hasty conclusions should not be driven from ¹⁸FDG uptake alone. However, an enlargement of the parotid gland with SUV_{max} > 4.7, and/or the presence of focal pulmonary lesions is highly suggestive of lymphoma (sensitivity 80%, specificity 83.3%) (90).

In summary, the advantages of PET/CT especially concern the screening of pSS patients for lymphoma (higher SUV max) and the guiding for diagnostic biopsy. PET/CT may also prove valuable for staging and assessing disease activity (91), but its usefulness is still limited for the diagnosis of pSS.

5. Conclusion

SGUS is a useful morphological tool for the diagnosis of pSS with well validated diagnostic performance and now with an OMERACT validated B-mode scoring. Its high availability and low cost makes it the imaging exam of choice in front-line clinical practice. In addition, severe heterogeneity of the salivary parenchyma could be a risk factor for progression to MALT lymphoma. Therefore, SGUS could be useful in selecting patients closer followup and surveillance for lymphomatous transition. CDUS, sensitive to change, could be a useful test to assess the activity of the disease and the impact of treatment on the salivary glands during pSS. Elastography, particularly the 2D-SWE technique, could be useful for the diagnosis of pSS at an early stage without morphological abnormalities in B-mode or to identify patients with suspected parotid MALT lymphoma. MRI of the salivary glands is the standard of care for patients with suspected parotid MALT lymphoma. PET should be considered cautiously during pSS due to lymphoma-free lymph node hypermetabolism even if gross parotid and/or pulmonary nodules hypermetabolism should suggest MALT lymphoma. Following this narrative review of the literature, we propose the **Figure 2** algorithm for the use of these different imaging examinations in clinical practice in the context of pSS syndrome.

Acknowledgements: The authors would like to thank Dr. Alain Lescoat, MD, PhD student, Department of Internal Medicine, University Hospital, Rennes, France, for his contribution to the proofreading of this narrative review.

Competing interests: No conflict of interest in relation to the results of this work is reported by all authors.

Funding: None

Practice points:

- Salivary glands ultrasonography (SGUS) typical feature is a positive argument in the diagnosis of sjögren syndrome among the other clinical, biological, immunological, and histological diagnosis criteria
- Salivary glands ultrasonography is helpful to diagnose sjögren syndrome in a sicca syndrome context
- A normal SGUS does not exclude the diagnosis of sjögren syndrome
- Assessing the vascularization of salivary glands should be helpful in evaluating Sjögren's disease activity

Research agenda

The OMERACT task force on Sjögren's syndrome assessed intra- and interreader reliability of consensus-based ultrasound definitions and scoring system using B-mode ultrasound videoclips and more recently in sjögren's patients. The next step of the Sjögren OMERACT working subgroup is to assess disease activity by evaluating the vascularization of the salivary glands using Doppler mode.

Reference

1. Vitali C, Bombardieri S, Jonsson R, Moutsopoulos HM, Alexander EL, Carsons SE, et al. Classification criteria for Sjögren's syndrome: a revised version of the European criteria proposed by the American-European Consensus Group. *Ann Rheum Dis.* 2002;61:554-558.
2. Shiboski SC, Shiboski CH, Criswell LA, Baer AN, Challacombe S, Lanfranchi H, et al. American College of Rheumatology classification criteria for Sjögren's syndrome: a data-driven, expert consensus approach in the Sjögren's International Collaborative Clinical Alliance Cohort. *Arthritis Care Res.* 2012;64:475-487.
3. Shiboski CH, Shiboski SC, Seror R, Criswell LA, Labetoulle M, Lietman TM, et al. 2016 American College of Rheumatology/European League Against Rheumatism classification criteria for primary Sjögren's syndrome: A consensus and data-driven methodology involving three international patient cohorts. *Ann Rheum Dis.* 2017;76(1):9-16.
4. Jousse-Joulin S, Milic V, Jonsson MV, Plagou A, Theander E, Luciano N, et al. Is salivary gland ultrasonography a useful tool in Sjögren's syndrome? A systematic review. *Rheumatology (Oxford).* 2016;55(5):789-800.
5. Mossel E, Delli K, van Nimwegen JF, Stel AJ, Haacke EA, Kroese FGM, et al. The parotid gland connection: ultrasound and biopsies in primary Sjögren's syndrome. *Ann Rheum Dis.* 2018;77(7):e38.
6. Carvajal Alegria G, Costa S, Jousse-Joulin S, Marcorelles P, Pers JO, Saraux A, et al. What is the agreement between pathological features of parotid gland and labial salivary gland biopsies? *Ann Rheum Dis.* 2018;77(7):e37.
7. Mossel E, Delli K, Arends S, Haacke EA, van der Vegt B, van Nimwegen JF, et al. Can ultrasound of the major salivary glands assess histopathological changes induced by treatment with rituximab in primary Sjögren's syndrome? *Ann Rheum Dis.* 2019;78(4):e27.
8. Devauchelle-Pensec V, Mariette X, Jousse-Joulin S, Berthelot JM, Perdriger A, Puéchal X, et al. Treatment of primary Sjögren syndrome with rituximab: a randomized trial. *Ann Intern Med.* 2014;160(4):233-42.
9. Cornec D, Costa S, Devauchelle-Pensec V, Chiche L, Saraux A, Pers JO. Do high numbers of salivary gland-infiltrating B cells predict better or worse outcomes after rituximab in patients with primary Sjögren's syndrome? *Ann Rheum Dis.* 2016 ;75(6):e33.
10. Theander E, Mandl T. Primary Sjögren's syndrome: diagnostic and prognostic value of salivary gland ultrasonography using a simplified scoring system. *Arthritis Care Res (Hoboken).* 2014;66(7):1102-7.

11. Coiffier G, Martel A, Albert JD, Lescoat A, Bleuzen A, Perdriger A, et al. Ultrasonographic damages of major salivary glands are associated with cryoglobulinemic vasculitis and lymphoma in primary Sjogren's syndrome: are the ultrasonographic features of the salivary glands new prognostic markers in Sjogren's syndrome? *Ann Rheum Dis.* 2019 Aug 16. pii: annrheumdis-2019-216122.
12. Jousse-Joulin S, D'Agostino MA, Nicolas C, Naredo E, Ohrndorf S, Backhaus M, et al. Video clip assessment of a salivary gland ultrasound scoring system in Sjögren's syndrome using consensual definitions: an OMERACT ultrasound working group reliability exercise. *Ann Rheum Dis.* 2019;78(7):967-973.
13. Damjanov N, Milic V, Nieto-González JC, Janta I, Martínez-Estupiñan L, Serrano B, et al. Multiobserver Reliability of Ultrasound Assessment of Salivary Glands in Patients with Established Primary Sjögren Syndrome. *J Rheumatol.* 2016;43(10):1858-1863.
14. Jousse-Joulin S, Devauchelle-Pensec V, Morvan J, Guías B, Pennec Y, Pers JO, et al. Ultrasound assessment of salivary glands in patients with primary Sjögren's syndrome treated with rituximab: Quantitative and Doppler waveform analysis. *Biologics.* 2007;1(3):311-9.
15. Jousse-Joulin S, Devauchelle-Pensec V, Cornec D, Marhadour T, Bressollette L, Gestin S, et al. Brief Report: Ultrasonographic Assessment of Salivary Gland Response to Rituximab in Primary Sjögren's Syndrome. *Arthritis Rheumatol.* 2015;67(6):1623-8.
16. Fisher BA, Everett CC, Rout J, et al. Effect of rituximab on a salivary gland ultrasound score in primary Sjögren's syndrome: results of the TRACTISS randomised double-blind multicentre substudy. *Ann Rheum Dis.* 2018;77(3):412–416.
17. De Vita S, Lorenzon G, Rossi G, Sabella M, Fossaluzza V. Salivary gland echography in primary and secondary Sjögren's syndrome. *Clin Exp Rheumatol* 1992;10: 351-56.
18. Arijji Y, Ohki M, Eguchi K et al. Texture analysis of sonographic features of the parotid gland in Sjogren's syndrome. *AJR Am J Roentgenol* 1996;166:935-41.
19. Jousse-Joulin S, Nowak E, Cornec D, Brown J, Carr A, Carotti M, et al. Salivary gland ultrasound abnormalities in primary Sjögren's syndrome: consensual US-SG core items definition and reliability. *RMD Open.* 2017;3(1):e000364.
20. Niemelä RK, Takalo R, Pääkkö E, Suramo I, Päivänsalo M, Salo T, Hakala M. Ultrasonography of salivary glands in primary Sjogren's syndrome. A comparison with magnetic resonance imaging and magnetic resonance sialography of parotid glands. *Rheumatology (Oxford).* 2004;43(7):875-9.
21. Salaffi F, Carotti M, Iagnocco A, Luccioli F, Ramonda R, Sabatini E, et al. Ultrasonography of salivary glands in primary Sjögren's syndrome: a comparison with contrast sialography and scintigraphy. *Rheumatology (Oxford).* 2008;47(8):1244-9.
22. Yonetsu K, Takagi Y, Sumi M, Nakamura T, Eguchi K. Sonography as a replacement for sialography for the diagnosis of salivary glands affected by Sjögren's syndrome. *Ann Rheum Dis.* 2002;61(3):276-7.
23. Song GG, Lee YH. Diagnostic accuracies of sialography and salivary ultrasonography in Sjögren's syndrome patients: a meta-analysis. *Clin Exp Rheumatol.* 2014;32(4):516-22.
24. Salaffi F, Argalia G, Carotti M, Giannini FB, Palombi C. Salivary gland ultrasonography in the evaluation of primary Sjögren's syndrome. Comparison with minor salivary gland biopsy. *J Rheumatol.* 2000;27(5):1229-36.
25. Mossel E, Arends S, van Nimwegen JF, Delli K, Stel AJ, Kroese FGM, et al. Scoring hypoechogenic areas in one parotid and one submandibular gland increases feasibility of ultrasound in primary Sjögren's syndrome. *Ann Rheum Dis.* 2018;77(4):556-562.
26. Abdel Razek AAK, Mukherji S. Imaging of sialadenitis. *Neuroradiol J.* 2017;30(3):205-215.
27. El Miedany YM, Ahmed I, Mourad HG, Mehanna AN, Aty SA, Gamal HM, et al. Quantitative ultrasonography and magnetic resonance imaging of the parotid gland: can they replace the histopathologic studies in patients with Sjogren's syndrome? *Joint Bone Spine.* 2004 Jan;71(1):29-38.
28. Hocevar A, Ambrozic A, Rozman B, Kveder T, Tomsic M. Ultrasonographic changes of major salivary glands in primary Sjogren's syndrome. Diagnostic value of a novel scoring system. *Rheumatology (Oxford).* 2005;44(6):768-72.
29. Milic VD, Petrovic RR, Boricic IV, Radunovic GL, Pejnovic NN, Soldatovic I, et al. Major salivary gland sonography in Sjögren's syndrome: diagnostic value of a novel ultrasonography score (0-12) for parenchymal inhomogeneity. *Scand J Rheumatol.* 2010;39(2):160-6.

30. Cornec D, Jousse-Joulin S, Pers JO, Marhadour T, Cochener B, Boisramé-Gastrin S, et al. Contribution of salivary gland ultrasonography to the diagnosis of Sjögren's syndrome: toward new diagnostic criteria? *Arthritis Rheum.* 2013;65(1):216-25.
31. Martel A, Coiffier G, Bleuzen A, Goasguen J, de Bandt M, Deligny C, et al. What is the best salivary gland ultrasonography scoring methods for the diagnosis of primary or secondary Sjögren's syndromes? *Joint Bone Spine.* 2019;86(2):211-217.
32. Zhang X, Zhang S, He J, Hu F, Liu H, Li J, et al. Ultrasonographic evaluation of major salivary glands in primary Sjögren's syndrome: comparison of two scoring systems. *Rheumatology (Oxford).* 2015;54(9):1680-7.
33. Qi X, Sun C, Tian Y, Han Y, Peng C, Jin H, et al. Comparison of the diagnostic value of four scoring systems in primary sjögren's syndrome patients. *Immunol Lett.* 2017;188:9-12.
34. Milic V, Petrovic R, Boricic I, Radunovic G, Marinkovic-Eric J, Jeremic P, et al. Ultrasonography of major salivary glands could be an alternative tool to sialoscintigraphy in the American-European classification criteria for primary Sjogren's syndrome. *Rheumatology (Oxford).* 2012;51(6):1081-5.
35. Le Goff M, Cornec D, Jousse-Joulin S, Guellec D, Costa S, Marhadour T, et al. Comparison of 2002 AECG and 2016 ACR/EULAR classification criteria and added value of salivary gland ultrasonography in a patient cohort with suspected primary Sjögren's syndrome. *Arthritis Res Ther.* 2017;19(1):269.
36. Cornec D, Jousse-Joulin S, Marhadour T, Pers JO, Boisramé-Gastrin S, Renaudineau Y, Salivary gland ultrasonography improves the diagnostic performance of the 2012 American College of Rheumatology classification criteria for Sjögren's syndrome. *Rheumatology (Oxford).* 2014;53(9):1604-7.
37. Takagi Y, Nakamura H, Sumi M, Shimizu T, Hirai Y, Horai Y, et al. Combined classification system based on ACR/EULAR and ultrasonographic scores for improving the diagnosis of Sjögren's syndrome. *PLoS One.* 2018;13(4):e0195113.
38. van Nimwegen JF, Mossel E, Delli K, van Ginkel MS, Stel AJ, Kroese FGM, et al. Incorporation of Salivary Gland Ultrasonography Into the American College of Rheumatology/European League Against Rheumatism Criteria for Primary Sjögren's Syndrome. *Arthritis Care Res (Hoboken).* 2020;72(4):583-590.
39. Geng Y, Li B, Deng X, Ji L, Zhang X, Zhang Z. Salivary gland ultrasound integrated with 2016 ACR/EULAR classification criteria improves the diagnosis of primary Sjögren's syndrome. *Clin Exp Rheumatol.* 2020;38(2):322–328.
40. Jousse-Joulin S, Gatineau F, Baldini C, Baer A, Barone F, Bootsma H, et al. Weight of salivary gland ultrasonography compared to other items of the 2016 ACR/EULAR classification criteria for Primary Sjögren's syndrome. *J Intern Med.* 2020;287(2):180-188.
41. Hammenfors DS, Brun JG, Jonsson R, Jonsson MV. Diagnostic utility of major salivary gland ultrasonography in primary Sjögren's syndrome. *Clin Exp Rheumatol.* 2015;33(1):56-62.
42. Zabotti A, Zandonella Callegger S, Gandolfo S, Valent F, Giovannini I, Cavallaro E, et al. Hyperechoic bands detected by salivary gland ultrasonography are related to salivary impairment in established Sjögren's syndrome. *Clin Exp Rheumatol.* 2019;37 Suppl 118(3):146-152.
43. Milic V, Colic J, Cirkovic A, Stanojlovic S, Damjanov N. Disease activity and damage in patients with primary Sjogren's syndrome: Prognostic value of salivary gland ultrasonography. *PLoS One.* 2019 Dec 31;14(12):e0226498.
44. Inanc N, Şahinkaya Y, Mumcu G, Türe Özdemir F, Paksoy A, Ertürk Z, et al. Evaluation of salivary gland ultrasonography in primary Sjögren's syndrome: does it reflect clinical activity and outcome of the disease? *Clin Exp Rheumatol.* 2019;37 Suppl 118(3):140-145.
45. Astorri E, Sutcliffe N, Richards PS, Suchak K, Pitzalis C, Bombardieri M, et al. Ultrasound of the salivary glands is a strong predictor of labial gland biopsy histopathology in patients with sicca symptoms. *J Oral Pathol Med.* 2016;45(6):450-4.
46. Mossel E, Delli K, van Nimwegen JF, Stel AJ, Kroese FGM, Spijkervet FKL, et al. Ultrasonography of major salivary glands compared with parotid and labial gland biopsy and classification criteria in patients with clinically suspected primary Sjögren's syndrome. *Ann Rheum Dis.* 2017;76(11):1883-1889.
47. Kim JW, Lee H, Park SH, Kim SK, Choe JY, Kim JK. Salivary gland ultrasonography findings are associated with clinical, histological, and serologic features of Sjögren's syndrome. *Scand J Rheumatol.* 2018;47(4):303-310.
48. Cornec D, Jousse-Joulin S, Costa S, Marhadour T, Marcorettes P, Berthelot JM, et al. High-Grade Salivary-Gland Involvement, Assessed by Histology or Ultrasonography, Is Associated with a Poor Response to a Single

- Rituximab Course in Primary Sjögren's Syndrome: Data from the TEARS Randomized Trial. *PLoS One*. 2016;11(9):e0162787.
49. Gazeau P, Cornec D, Jousse-Joulin S, Guellec D, Saraux A, Devauchelle-Pensec V. Time-course of ultrasound abnormalities of major salivary glands in suspected Sjögren's syndrome. *Joint Bone Spine*. 2018;85(2):227-232.
 50. Carotti M, Salaffi F, Manganelli P, Argalia G. Ultrasonography and colour doppler sonography of salivary glands in primary Sjögren's syndrome. *Clin Rheumatol*. 2001;20(3):213-9.
 51. Shimizu M, Okamura K, Yoshiura K, Ohyama Y, Nakamura S. Sonographic diagnosis of Sjögren syndrome: evaluation of parotid gland vascularity as a diagnostic tool. *Oral Surg Oral Med Oral Pathol Oral Radiol Endod*. 2008;106(4):587-94.
 52. Chikui T, Yonetsu K, Izumi M, Eguchi K, Nakamura T. Abnormal blood flow to the submandibular glands of patients with Sjögren's syndrome: Doppler waveform analysis. *J Rheumatol*. 2000;27(5):1222-8.
 53. Martinoli C, Derchi LE, Solbiati L, Rizzatto G, Silvestri E, Giannoni M. Color Doppler sonography of salivary glands. *AJR Am J Roentgenol*. 1994;163(4):933-41.
 54. Lee KA, Lee SH, Kim HR Diagnostic and predictive evaluation using salivary gland ultrasonography in primary Sjögren's syndrome. *Clin Exp Rheumatol*. 2018;36 Suppl 112(3):165-172.
 55. Giuseppetti GM, Argalia G, Salera D, Ranaldi R, Danieli G, Cappelli M. Ultrasonographic contrast-enhanced study of sicca syndrome. *Eur J Radiol*. 2005;54(2):225-32.
 56. Hočvar A, Jousse-Joulin A, Perko N, Finzel S, Hanova P, Iagnocco A, et al. Assessing the vascularization of salivary glands in patients with Sjögren's syndrome - the OMERACT US subtask group reliability exercise. [abstract]. *Arthritis Rheumatol*. 2019; 71 (suppl 10). <https://acrabstracts.org/abstract/assessing-the-vascularization-of-salivary-glands-in-patients-with-sjogrens-syndrome-an-omeract-ultrasound-group-reliability-exercise/>. Accessed April 19, 2020.
 57. Gennisson JL, Deffieux T, Fink M, Tanter M. Ultrasound elastography: principles and techniques. *Diagn Interv Imaging*. 2013;94(5):487-95.
 58. Sigrist RMS, Liao J, Kaffas AE, Chammas MC, Willmann JK. Ultrasound Elastography: Review of Techniques and Clinical Applications. *Theranostics*. 2017;7(5):1303-1329.
 59. Dejaco C, De Zordo T, Heber D, et al. Real-time sonoelastography of salivary glands for diagnosis and functional assessment of primary Sjögren's syndrome. *Ultrasound Med Biol*. 2014;40:2759-2767.
 60. Gunes Tatar I, Altunoglu H, Kurt A, Altunoglu A, Ozturk MA, Erten S, et al. The role of salivary gland elastosonography in Sjögren's syndrome: preliminary results. *Int J Rheum Dis*. 2014 Nov;17(8):904-9.
 61. Knopf A, Hofauer B, Thurmle K, et al. Diagnostic utility of acoustic radiation force impulse (ARFI) imaging in primary Sjögren's syndrome. *Eur Radiol*. 2015;25:3027-3034
 62. Samier-Guérin A, Saraux A, Gestin S, Cornec D, Marhadour T, Devauchelle-Pensec V, et al. Can ARFI elastometry of the salivary glands contribute to the diagnosis of Sjögren's syndrome? *Joint Bone Spine*. 2016;83(3):301-6.
 63. Zhang S, Zhu J, Zhang X, He J, Li J. Assessment of the stiffness of major salivary glands in primary Sjögren's syndrome through quantitative acoustic radiation force impulse imaging. *Ultrasound Med Biol*. 2016;42:645-653.
 64. Hofauer B, Mansour N, Heiser C, et al. Sonoelastographic modalities in the evaluation of salivary gland characteristics in Sjögren's syndrome. *Ultrasound Med Biol*. 2016;2016(42):2130-2139.
 65. Chen S, Wang Y, Chen S, Wu Q, Chen S. Virtual touch quantification of the salivary glands for diagnosis of primary sjögren syndrome. *J Ultrasound Med*. 2016;35(12):2607-2613.
 66. Turnaoglu H, Kural Rahatli F, Pamukcu M, Haberal KM, Uslu N. Diagnostic value of acoustic radiation force impulse imaging in the assessment of salivary gland involvement in primary Sjögren's syndrome. *Med Ultrason*. 2018;20(3):313-318.
 67. Cindil E, Oktar SO, Akkan K, Sendur HN, Mercan R, Tufan A, et al. Ultrasound elastography in assessment of salivary glands involvement in primary Sjögren's syndrome. *Clin Imaging*. 2018;50:229-234.
 68. Pia LJ, Juan BM, Frank P, Angela AA, Jose G, Juan de Dios BS. Is sonoelastography a helpful method of evaluation to diagnose Sjögren's syndrome? *Int J Rheum Dis*. 2019;22(2):175-181.

69. Arslan S, Durmaz MS, Erdogan H, Esmen SE, Turgut B, Iyiso MS. Two-Dimensional Shear Wave Elastography in the Assessment of Salivary Gland Involvement in Primary Sjögren's Syndrome. *J Ultrasound Med.* 2019 Nov 25. doi: 10.1002/jum.15179.
70. Bădărină M, Serban O, Maghear L, Bocsa C, Micu M, Damian L, et al. Shear wave elastography as a new method to identify parotid lymphoma in primary Sjögren Syndrome patients: an observational study. *Rheumatol Int.* 2020 Mar 21. doi: 10.1007/s00296-020-04548-x.
71. La Paglia GMC, Sanchez-Pernaute O, Alunno A, et al. Ultrasound salivary gland involvement in Sjogren's syndrome vs. other connective tissue diseases: is it autoantibody and gland dependent?. *Clin Rheumatol.* 2020;39(4):1207–1215.
72. Coiffier G, Jousse-Joulin S, Cornec D, Garlantézec R, Bleuzen A, Diot E, et al. Ultrasonographic salivary gland evaluation in systemic sclerosis: is sicca syndrome secondary to an authentic overlap syndrome or another specific fibrotic manifestation of the disease? *Ann Rheum Dis.* 2019 Jul 12;annrheumdis-2019-215972.
73. Couderc M, Tournadre A, Mathieu S, Pereira B, Soubrier M, Dubost JJ. Do the salivary glands of patients with systemic sclerosis show ultrasonographic modifications suggestive of Sjögren's syndrome? *Ann Rheum Dis.* 2019 Jun 12. pii: annrheumdis-2019-215777.
74. Law ST, Jafarzadeh SR, Govender P, Sun X, Sancherawala V, Kissin EY. Comparison of Ultrasound Features of Major Salivary Glands in Sarcoidosis, Amyloidosis, and Sjögren's Syndrome. *Arthritis Care Res (Hoboken).* 2019 Jul 15. doi: 10.1002/acr.24029.
75. Narayan AK, Baer A, Fradin J. Sonographic findings of IgG4-related disease of the salivary glands: Case report and review of the literature. *J Clin Ultrasound.* 2018;46(1):73–77.
76. Shimizu, M., Okamura, K., Kise, Y. et al. Effectiveness of imaging modalities for screening IgG4-related dacryoadenitis and sialadenitis (Mikulicz's disease) and for differentiating it from Sjögren's syndrome (SS), with an emphasis on sonography. *Arthritis Res Ther.* 2015;17 :223.
77. Liu Y, Xue M, Wang Z, et al. Salivary gland involvement disparities in clinical characteristics of IgG4-related disease: a retrospective study of 428 patients. *Rheumatology (Oxford).* 2020;59(3):634–640.
78. Izumi M, Eguchi K, Ohki M, Uetani M, Hayashi K, Kita M, et al. MR Imaging of the Parotid Gland in Sjögren's Syndrome: A Proposal for New Diagnostic Criteria. *AJR Am J Roentgenol.* 1996 ;166(6) :1483-7.
79. Tonami H, Ogawa Y, Matoba M, et al. MR sialography in patients with Sjögren syndrome. *AJNR Am J Neuroradiol.* 1998;19(7):1199–1203.
80. Zhu L, Zhang C, Hua Y, Yang J, Yu Q, Tao X, Zheng J. Dynamic contrast-enhanced MR in the diagnosis of lympho-associated benign and malignant lesions in the parotid gland. *Dentomaxillofac Radiol.* 2016;45(4):20150343.
81. Zheng N, Li R, Liu W, Shao S, Jiang S. The diagnostic value of combining conventional, diffusion-weighted imaging and dynamic contrast-enhanced MRI for salivary gland tumors. *Br J Radiol.* 2018;91(1089):20170707.
82. Kojima I, Sakamoto M, Ikubo M, et al. Diagnostic performance of MR imaging of three major salivary glands for Sjögren's syndrome. *Oral Dis.* 2017;23(1):84–90.
83. Niemela RK, Paakko E, Suramo I, Takalo R, Hakala M. Magnetic resonance imaging and magnetic resonance sialography of parotid glands in primary Sjogren's syndrome. *Arthritis Rheum.* 2001;45(6):512-518
84. Takagi Y, Sumi M, Sumi T, Ichikawa Y, Nakamura T. MR microscopy of the parotid glands in patients with Sjogren's syndrome: quantitative MR diagnostic criteria. *AJNR Am J Neuroradiol.* 2005;26(5):1207-14.
85. Tonami H, Higashi K, Matoba M, Yokota H, Yamamoto I, Sugai S. A comparative study between MR sialography and salivary gland scintigraphy in the diagnosis of Sjögren syndrome. *J Comput Assist Tomogr.* 2001;25(2):262-8.
86. Yokosawa M, Tsuboi H, Nasu K, Hagiya C, Hagiwara S, Hirota T, et al. Usefulness of MR imaging of the parotid glands in patients with secondary Sjögren's syndrome associated with rheumatoid arthritis. *Mod Rheumatol.* 2015;25(3):415-20.
87. Zhu L, Wang P, Yang J, Yu Q. Non-Hodgkin lymphoma involving the parotid gland: CT and MR imaging findings. *Dentomaxillofac Radiol.* 2013;42(9):20130046.
88. Kato H, Kanematsu M, Goto H, Mizuta K, Aoki M, Kuze B, et al. Mucosa-associated lymphoid tissue lymphoma of the salivary glands: MR imaging findings including diffusion-weighted imaging. *Eur J Radiol.* 2012;81(4):e612-7.

89. Zhu L, Zhang C, Hua Y, Yang J, Yu Q, Tao X, Zheng J. Dynamic contrast-enhanced MR in the diagnosis of lympho-associated benign and malignant lesions in the parotid gland. *Dentomaxillofac Radiol.* 2016;45(4):20150343.
90. Keraen J, Blanc E, Besson FL, Leguern V, Meyer C, Henry J, Belkhir, et al. Usefulness of ¹⁸F-Labeled Fluorodeoxyglucose–Positron Emission Tomography for the Diagnosis of Lymphoma in Primary Sjögren's Syndrome. *Arthritis Rheumatol.* 2019;7:1147-1157.
91. Cohen C, Mekinian A, Uzunhan Y, Fauchais AL, Dhote R, Pop G, et al. 18F-fluorodeoxyglucose positron emission tomography/computer tomography as an objective tool for assessing disease activity in Sjögren's syndrome. *Autoimmun Rev.* 2013;12(11):1109-14.

Best Practice & Research Clinical Rheumatology

Current status of imaging of Sjogren's syndrome.

Sandrine Jousse-Joulin, Guillaume Coiffier.

Tables & Figures

Table 1. Different systems of SGUS scoring for a Sjogren diagnosis.

Table 2. Elastography diagnostic performance of major salivary glands during pSS.

Table 3. Ultrasound aspects and clinical, biological and histological features observed in Sjogren's syndrome and other inflammatory disorders of major salivary gland.

Table 4. MR Imaging diagnostic performance of major salivary glands during pSS.

Figure 1. OMERACT scoring system of SGUS in pSS.

Figure 2. Algorithm of strategy for the use of imaging exams during Sjogren's syndrome in clinical practice.

Table1. Different systems of US-SG scoring for a primary Sjogren's syndrome diagnosis

Articles	Definition of the scoring	System of scoring	Diagnosis performance for pSS
DeVita ¹ (1992)	Mild Inhomogeneity (1 point, just for PGs): diffuse or localized micro-alveolar structure) Evident Inhomogeneity (2 points): evident multiple scattered hypo-echogenic areas, usually of variable size and not uniformly distributed, and/or multiple punctate ir linear non-shadowing densities) Gross Inhomogeneity (3 points): large circumscribed or confluent hypoechoogenic areas, and/or gross linear densities, and/or multiple cysts or multiple calcifications) Sum of the (0-3) single scores for each couple of PG and SMG. If discordant result for homonymous glands, the higher degree should be considered.	0-6	Abnormal score ≥ 1 Se 88.8%, Sp 84.6% (single center of cohort, 27 pSS vs 90 controls) ¹
Ariji ² (1996)	Sonographic grading was based on gland contour and internal echoes of the PGs gland Grade 0: Regular contours with no internal echoes. Grade 1: Regular contours with small multiple hypochoic spots/areas without echogenic bands. Grade 2: Regular contours with round multiple hypochoic spots/areas without echogenic bands. Grade 3: Irregular contours with round multiple hypochoic spots/areas with echogenic bands. Grade 4: Irregular contours with irregular multiple hypochoic spots/areas with echogenic bands. The final score was the highest score in any of the PGs.	0-4	Abnormal score Se 68.0%, Sp 82.0% (single center of Nagasaki cohort between June 1993 and May 2009, 188 pSS vs 172 controls) ¹⁰
Salaffi ³ (2000)	DeVita score simplified by Salaffi. Grade 0: Normal glands Grade 1: Regular contour, small hypochoic spots/areas, without echogenic bands, regular or increased glandular volume (mean values 20 + 3 mm for the parotids and 13 + 2 mm for the submandibular glands) and ill-defined posterior glandular border (definite echogenic border with respect to the neighbouring structures). Grade 2: Regular contour, evident multiple scattered hypoechoogenic areas usually of variable size (<2 mm) and not uniformly distributed, without echogenic bands, regular or increased glandular volume and ill-defined posterior glandular border. Grade 3: Irregular contour, multiple large circumscribed or confluent hypoechoogenic areas (2-6 mm) and/or multiple cysts, with echogenic bands, regular or decreased glandular volume and no visible posterior glandular border. Grade 4: Irregular contour, multiple large circumscribed or confluent hypoechoogenic areas (>6 mm), and/or multiple cysts or multiple calcifications, with echogenic bands, resulting in severe damage to the glandular architecture, decreased glandular volume and posterior glandular border not visible. The final score is the sum of the scores of each gland.	0-16	Abnormal score ≥ 7 Se 75.3, Sp 83.5% (single center of Roma cohort, 77 pSS vs 79 controls) ¹¹ Se 63.2%, Sp 94.4% (French multi-center cohort, 39 pSS vs 36 controls) ¹² Se 80.0%, Sp 93.0% (single center of Beijing cohort, 105 pSS vs 57 controls) ¹³ Abnormal score ≥ 5 Se 90.3%, Sp 87.2% (Chinese cohort, 134 pSS vs 109 controls) ¹⁴
El Miedany ⁴ (2004)	Sonographic grading was based on inhomogeneity of the PGs gland Grade 0: Normal homogenous parenchyma. Grade 1: Mild PIH seen as diffuse hypochoic areolae less than 2 mm with blurred borders. Grade 2: Moderate PIH seen as large hypochoic areas, 2-6 mm diameter, with sharp borders. Grade 3: Severe PIH with large, more than 6 mm circumscribed hypochoic areas.	0-3	Abnormal score ≥ 1 Se 95.7%, Sp 92.7% (single center of Cairo cohort, 47 pSS vs 40 controls) ⁴
Hocevar ⁵ (2005)	Echogenicity : 0-1 (lower than the thyroid) Homogeneity : 0-3 (Grading 0 was for a homogeneous gland, 1 for mild inhomogeneity, 2 for evident inhomogeneity, and 3 for a grossly inhomogeneous gland.) Presence of hypoechoic areals : 0-3 (grade 0, absent; grade 1, a few, scattered; grade 2, several; grade 3, numerous hypoechoic areas). Hyperechoic reflections : 0-3 in the parotid glands (grade 0, absent; grade 1, a few, scattered; grade 2, several; grade 3, numerous hyperechoic reflections) and from 0 (absent) to 1 (present) in the submandibular glands. Clearness of salivary gland borders : 0-3 (grade 0, clear, regular defined borders; grade 1, partly defined borders; grade 2, ill-defined borders; grade 3, borders not visible).	0-48	Abnormal score ≥ 17 Se 62.8%, Sp 95.0% (single center of Lubjuna cohort, 68 pSS vs 150 controls) ⁵ Se 63.2%, Sp 91.7% (French multi-center cohort, 39 pSS vs 36 controls) ¹³ Abnormal score ≥ 15 Se 88.6%, Sp 84.2% (single center of Beijing cohort, 105 pSS vs 57 controls) ¹⁴
Milic ⁶ (2010)	Parenchymal inhomogeneity was graded from 0 to 3, from homogeneous parenchyma to grossly inhomogeneous gland (mild parenchymal inhomogeneity, grade 1, was treated as a normal finding).	0-12	Abnormal score ≥ 6 Se 95.1%, Sp 90.0% (single center of Belgrade cohort, 115 pSS vs 86 controls) ⁶
Cornec ⁷ (2013)	DeVita score simplified by Jousse-Joulin : grade 0: normal homogeneous glands; grade 1: small hypoechoic areas without echogenic bands; grade 2: multiple hypoechoic areas measuring < 2 mm with echogenic bands; grade 3: multiple hypoechoic areas measuring 2-6 mm with hyperechoic bands; grade 4: multiple hypoechoic areas measuring > 6 mm or multiple calcifications with echogenic bands. PGs and SMGs was evaluated. The worst score was considered for the scoring.	0-4	Abnormal score ≥ 2 Se 62.8%, Sp 95.0% (single center of Brest cohort, 78 pSS vs 80 controls) ⁷ Se 65.8%, Sp 94.4% (French multi-center cohort, 39 pSS vs 36 controls) ¹³
Theander ⁸ (2014)	Simplified score inspired by Milic with better definition grade 2 and 3. Grade 0: completely homogeneous, Grade 1: mildly inhomogeneous, Grade 2: several rounded hypochoic lesions were present. Finally, if the rounded hypochoic lesions were either numerous or confluent, a score of 3 was given. The final score was the highest score in any of the 4 salivary glands.	0-3	Abnormal score ≥ 2 Se 52.0%, Sp 98.5% (Swedish cohort, 105 pSS vs 57 controls) ⁸ Se 90.3%, Sp 83.5% (Chinese cohort, 134 pSS vs 109 controls) ¹³
Jousse-Joulin ⁹ (2019)	OMERACT US-SG scoring Quantitative scoring for gland parenchyma inhomogeneity: grade 0: normal parenchyma grade 1: minimal change: mild inhomogeneity without anechoic/hypochoic areas grade 2: moderate change: moderate inhomogeneity with focal anechoic/hypochoic areas but surrounded with normal tissue grade 3: severe change: diffuse inhomogeneity with focal anechoic/hypochoic areas occupying the entire gland surface but surrounded with no normal tissue Specific qualitative scoring pattern : Fatty gland (grade 1) : Diffuse homogeneity with hyperechoic gland compared with adjacent tissue Fibrous gland (grade 3) : Hyperechoic bands developed into fibrotic tissue indistinguishable from the adjacent soft tissue PGs and SMGs was evaluated. The worst score was considered for the scoring.	0-3	Abnormal score ≥ 2

Table 2. Elastography diagnostic performance of major salivary glands during pSS.

Articles	Patients	Technique	Results
Dejaco C (2014)	45 pSS 35 controls	RTTE ACUSON Antares Siemens	RTTE 6.5 [2-13] vs 4.0 [1-9], $p < 0.001$ RTTE ≥ 6 , Se 66.7%, Sp 85.7%
Gunes Tatar (2014)	23 pSS (ACR2012) 20 controls	RTTE MyLAB60 Esaote	elasticity scores of the PGs and SMGs did not show a statistically significant difference between patients with pSS and controls ($P > 0.05$).
Knopf (2015)	70 pSS (AECG) 87 controls	ARFI ACUSON S2000 Siemens	PGs (SWV: 2.86 ± 0.07 vs 1.87 ± 0.02 , $p < 0.001$) Cut-off ≥ 2.4 m/s, Se 77%, Sp 56% SMGs (SWV: 2.10 ± 0.07 vs 1.81 ± 0.02 , $p < 0.001$)
Samier-Guerin (2016)	10 pSS (ACR2012) 15 controls	ARFI ACUSON S2000 Siemens	PGs (SWV: 2.34 ± 0.32 vs 1.79 ± 0.38 , $p < 0.001$) SMGs (SWV: 1.81 ± 0.31 vs 1.77 ± 0.19 , $p = 0.89$)
Zhang (2016)	21 pSS (AECG) 11 controls	ARFI ACUSON S3000 Siemens	PGs (VTQ: 1.33 ± 0.22 vs 1.18 ± 0.04 , $p < 0.01$) SMGs (VTQ: 1.27 ± 0.17 vs 1.19 ± 0.07 , $p = 0.09$)
Hofauer (2016)	50 pSS (AECG) 50 controls	Comparison between 2 techniques RTTE <i>vs</i> ARFI	PGs (SWV: 2.99 ± 0.96 vs 2.16 ± 0.71 , $p < 0.001$) Cut-off ≥ 2.34 m/s, Se 77%, Sp 57.8% SMGs (SWV: 2.54 ± 0.76 vs 2.04 ± 0.40 , $p = 0.008$) Cut-off ≥ 1.95 m/s, Se 63%, Sp 46.2%
Chen (2016)	54 pSS (AECG) 74 controls	ARFI ACUSON S2000 Siemens	PGs (SWV: 2.78 ± 0.82 vs 1.85 ± 0.31 , $p < 0.001$) Cut-off ≥ 2.18 m/s, Se 89.3%, Sp 75.3% SMGs (SWV: 2.25 ± 0.34 vs 1.82 ± 0.27 , $p < 0.001$) Cut-off ≥ 2.15 m/s, Se 77.1%, Sp 85.4%
Turnaoglu (2018)	25 pSS (ACR2016) 25 controls	ARFI ACUSON S3000 Siemens	PGs (SWV: 2.6 ± 0.48 vs 1.78 ± 0.15 , $p < 0.001$) Cut-off ≥ 1.93 m/s, Se 92.0%, Sp 92.0% SMGs (SWV: 2.2 ± 0.28 vs 1.80 ± 0.14 , $p < 0.001$) Cut-off ≥ 1.98 m/s, Se 84.0%, Sp 92.0%
Cindil (2018)	58 pSS (AECG) 25 controls	RTTE EUB7500 Hitachi	PGs (Stain ratio: 3.54 vs 2.17 , $p < 0.001$) Cut-off ratio ≥ 2.6 , Se 79%, Sp 96% SMGs (Stain ratio: 2.21 vs 1.31 , $p < 0.001$) Cut-off ratio ≥ 2.7 , Se 74%, Sp 96%
Pia (2019)	41 pSS (AECG) 47 controls	ARFI ACUSON S2000 Siemens	PGs (SWV: 2.09 ± 0.67 vs 1.23 ± 0.12 , $p < 0.001$) Cut-off ≥ 1.75 , Se 75.6%, Sp 50.0% SMGs (SWV: 2.25 ± 0.46 vs 1.57 ± 0.13 , $p < 0.001$) Cut-off ≥ 2.0 , Se 69.0%, Sp 44.0%
Arslan (2019)	53 pSS 30 controls	2D SWE APLIO500 Toshiba	PGs (SWV: 3.1 ± 0.8 vs 2.1 ± 0.3 , $p < 0.001$) Cut-off ≥ 2.48 , Se 82.1%, Sp 91.7% SMGs (SWV: 2.9 ± 0.4 vs 2.3 ± 0.2 , $p < 0.001$) Cut-off ≥ 2.59 , Se 79.2%, Sp 90.0%
Bădărinză (2020)	51 pSS (ACR2016) with 8 NHL 35 controls	2D SWE AixplorerUltimate SuperSonic Imagine	PGs SWE ≥ 6.45 kPa Se 58.6%, Sp 80.0% If only Grade 0-1 considered, diagnosis in 94.3% In NHL group 13.9 kPa vs 6.3 kPa, $p < 0.001$ If SWE > 11.5 kPa in $> 50\%$ hyperechoic band and parotidomegaly MALT lymphoma diagnosis with Se 92%, Sp 100%.

RTTE: Real-Time Tissue Elastography, ARFI: Acoustic Radiation Force Impulse, SWV: Shear Wave Velocity, VTQ: Virtual Touch tissue Quantification.

Table 3. Ultrasound aspects and clinical, biological and histological features observed in Sjögren's syndrome and other inflammatory disorders of major salivary gland.

	SGUS	Clinical	Biological	MSGB	Others/Complication
Sjogren Syndrome^a	Combined involvement of the all major SGs with a heterogeneous parenchyma with numerous pseudocysts/ hyperechogenic bands. Enlarged PGs must suggest a lymphomatous complication.	Sicca syndrome Asthenia/pain Recurrent parotidomegaly Abnormal salivary flow	SSA antibodies ^b RF without ACPA ^c p.c. hyperG	Lymphocyte infiltr. Focus score $\geq 1/4$	Cytopenia Interstitial lung disease Interstitial nephropathy with tubular acidosis Purpura, cryoglobulinemia Peripheral neuropathy CNS involvement Others auto-immune diseases
Sarcoidosis	Nodal enlargement to diffuse or partial involvement of the PG with various degrees of echogenicity. Hypertrophic PGs.	Heerford syndrome (parotidomegaly with facial nerve palsy and uveitis) Mickuliz syndrom	No auto-immunity p.c. hyperG hypercalcemia elevated ACE	non-caseating granuloma	Thoracic involvement CNS involvement Liver and spleen enlargement Lymphadenopathy Subcutaneous nodules
AL Amyloidosis	Hypoechoic lesions and hyperechoic septa similar in appearance to Sjogren.	Asthenia/pain Carpian-tunnel syndrome Eyelid swelling, purpura around the eyes ("raccoon-eyes") Tongue swelling	No auto-immunity m.c. hyperG kappa/lambda ratio abnormalites	Positive staining on Congo red	Heart Faillure Nephrotic syndrome Peripheral neuropathy
IgG4-related disease	Hypertrophic gland with hypoechoic lesions (pseudocyst) involving preferentially the SMGs (90%) with common sparing of the PGs (< 35%) <i>and/or</i> Reticular pattern (alternating hyperechogenic areas surrounded by hyperechogenic band with "honeycomb" appearance) <i>and/or</i> Nodular pattern (hypoechoic mass distorting the contours of the gland) (60%)	SG tumefaction before sicca syndrom	No auto-immunity p.c. hyperG IgG4 $\geq 1.35\text{g/L}$ Eosinophila <i>and/or</i> IgE possible	Plasmocytes infiltr. Ratio Plasm _{IgG4/IgG+} > 40%	Periorbital involvement Lymphadenopathy Pancreatitis Cholangitis Retroperitoneal fibrosis
Chronic Obstructive sialadenitis	Must be suggest if only one SG (especially PG) is involved with normal aspect of the others SG. Variable SGUS findings depending on the severity and duration of inflammation. heterogeneous parenchyma with numerous pseudocysts and hyperechogenic bands (Sjogren's like aspect) Irregularly enlarged (sausage-shaped) main duct with central dilation tapering to normal peripheral ducts is characteristic of recurrent COS. Surch stones.	Recurrent painful acute parotidomegaly without sicca syndrom	No auto-immunity No p.c. hyperG	normal	CT (stones) or MR sialography (duct stenosis)

^a primary SS, secondary SS or Sjogren-like syndrome (i.e. Human Immunodeficiency Virus, Hepatitis C Virus, graft versus host disease), bSSA antibodies without others nuclear antibodies (except SSB antibodies) suggest Sjogren syndrome, but if associated to DNA/Sm antibodies, investigate systemic lupus (according to clinical presentation) ^c RF with ACPA must suggest secondary SS associated to Rheumatoid Arthritis, PG: Parotid Gland, SMG: SubMandibular Gland, MSGB: Minor salivary gland biopsy, p.c.hyperG: polyclonal hypergammaglobulinemia, ACE: Angiotensin-Converting Enzyme

Table 4. MR Imaging diagnostic performance of major salivary glands during Sjögren's Syndrome

Articles	Patients	Technique	Results	
Niemelä (2001)	29 pSS (AECG) 7 controls	MR imaging MR sialography	PGs (Se 81%, Sp 100%) PGs (Se 96%, Sp 100%)	Association with anti-SSA, repeated parotid swellings
Takagi (2005)	55 pSS (AECG) 28 controls (sicca syndrom)	MR imaging ≥ 5% <i>Fat area</i> < 90% <i>Lobule area</i> MR sialography ≥ 6 <i>sialolactatic foci</i> ≥ 5% <i>Fat area</i> + ≥ 6 <i>sialolactatic foci</i>	PGs Se 92.7%, Sp 89.3% Se 92.7%, 100% PGs Se 80.0%, Sp 100% Se 96.4%, Sp 100%	
Kojima (2017)	45 pSS (AECG) 24 controls (sicca syndrom)	MR imaging MR sialography	PGs (Se 67%, Sp 75%) SMGs (Se 58%, Sp 88%) SLGs (Se 33%, Sp 83%) PGs (Se 83%, Sp 83%) SMGs (Se 22%, Sp 100%) SLGs (Se 49%, Sp 83%)	SMGs, but not that of the PG or SLG, was smaller in patients with Sjögren's syndrome

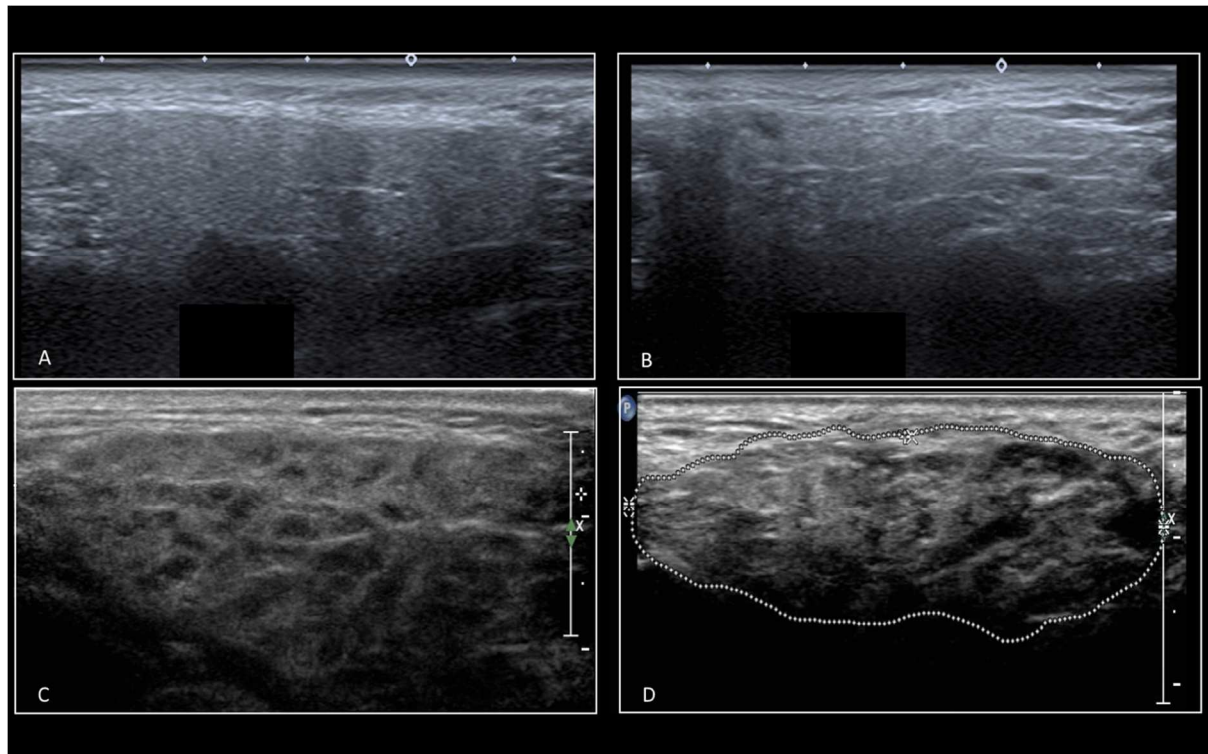


Figure 1. OMERACT scoring system of the SGUS in Sjogren's Syndrome.

Longitudinal scan of parotid gland with (A) normally homogeneous aspect (like thyroid parenchyma) (Grade 0), (B) non-specific heterogeneous aspects with few hypoechoic areas, few hyperechoic bands surrounded by normal parenchyma (Grade 1), (C) pathological moderate heterogeneous aspect with numerous hypoechoic area and hyperechoic bands but with few normal parenchymal areas (Grade 2) and (D) pathological severe heterogeneous aspect without normal parenchyma. There are no visible contours of the gland with decreased glandular volume. (12)